PERTURBATION OF A TURBULENT LIQUID FLOW BY THE BED-LOAD TRANSPORT OF GRANULAR MATTER

Fabíola Tocchini de Figueiredo, fabiolatdef@yahoo.com.br
Guilherme Augusto Ayek, guilhermeayek@hotmail.com
Eugênio Spanó Rosa, erosa@fem.unicamp.br
Faculdade de Engenharia Mecânica – Universidade Estadual de Campinas

Erick de Moraes Franklin, erick@unifei.edu.br
Instituto de Engenharia Mecânica – Universidade Federal de Itajubá

Abstract. *The transport of granular matter by a fluid flow is frequently found in nature and in industry. It is present, for example, in the erosion of river banks, in the displacement of desert dunes and on the transport of sand in hydrocarbon pipelines. The transport mechanism is the momentum transfer from the fluid flow to the grains. When the forces exerted by the fluid flow on a granular bed are able to move some grains, but are relatively small compared to the grains weight, the flow is not able to transport grains as a suspension. Instead, a mobile layer of grains known as bed-load takes place in which the grains stay in contact with the fixed part of the granular bed. If the fluid is a liquid, the thickness of this mobile layer is only a few grain diameters. The momentum transfer from the fluid flow to the mobile granular layer alters the fluid flow itself: the fluid flow is different from that that would exist if the bed were static. In this work we are interested in quantifying the changes (perturbation) caused by a mobile layer of grains (granular transport as bed-load) on a turbulent liquid flow. An experimental loop was built to allow bed-load transport and a PIV (Particle Image Velocimetry) device was used to measure the turbulent water flow over fixed and mobile granular beds. The spatial resolution of the measurements allows the experimental quantification of this perturbation and comparison with bed-load theories. To the authors' knowledge, this is the first time that this perturbation is experimentally measured in the case of turbulent flows of liquids.*

Keywords*: Turbulent flow, perturbation, sediment transport, bed-load*

1. INTRODUCTION

The transport of granular matter entrained by a fluid flow is frequently found in nature and in industry. It is present, for example, in the erosion of river banks, in the displacement of desert dunes and on the transport of sand in hydrocarbon pipelines. A better knowledge of this kind of transport is of great importance to understand nature and to improve human activities.

When shear stresses exerted by the fluid flow on the granular bed are able to move some grains, but are relatively small compared to the grains weight, the flow is not able to transport grains as a suspension. Instead, a mobile layer of grains known as bed-load takes place in which the grains stay in contact with the fixed part of the granular bed. The thickness of this mobile layer (called also *saltation* layer) is a few grain diameters (Bagnold, 1941; Raudkivi, 1976; Yalin, 1977).

Bed-load existence depends on the balance of two forces:

a) an entraining force, of hydrodynamic nature, proportional to τd^2, where τ is the shear stress on the bed and d is the mean grain diameter;

b) a resisting force, in this case related to the grains weight, proportional to $(\rho_s - \rho)gd^3$, where ρ is the density of the fluid, ρ_s is the density of the grains and g is the gravitational acceleration.

One relevant dimensionless parameter is the Shields number θ, which is the hydrodynamic force to weight ratio

$$\theta = \frac{\tau}{(\rho_s - \rho)gd} \tag{1}$$

and bed-load takes place for $O(0.01) < \theta < O(1)$. For a turbulent boundary-layer (like the one over a granular bed), $\tau = \rho u_*^2$, where u_* is the shear velocity. For a developed two dimensional turbulent boundary-layer over a granular bed

$$u^+ = \frac{1}{\kappa}\ln\left(\frac{y}{y_0}\right) = \frac{1}{\kappa}\ln\left(y^+\right) + B \tag{2}$$

where κ is the Kármán constant (we consider here $\kappa=0.41$) , y_0 is the roughness height, $u^+ = u/u_*$ (u is the velocity profile), $y^+ = yu_*/\nu$ is the transversal distance normalized by the viscous length (ν is the kinematic viscosity) and B is a constant. Although the two parts (after the first equal sign) of Eq. (2) are equivalent, the left part is generally employed in hydraulic rough case, while the right part is employed in hydraulic smooth cases. In the latter case, $B=5.5$.

The other relevant parameter is the Particular Reynolds number Re_*, which is the Reynolds number of the fluid at the grain scale. It relates the fluid inertia to the fluid viscosity terms at the grain scale

$$\mathrm{Re}_* = \frac{\rho u_* d}{\mu} \tag{3}$$

where u_* also represents the characteristic velocity of the fluid at the grain scale (shear velocity), d is the characteristic length at the grain scale (grain diameter) and μ is the liquid dynamic viscosity.

Some characteristics of the granular transport are obtained from these dimensionless parameters. The Shields number θ can show if the bed-load is strong or weak, and the Particular Reynolds number Re_* determines if the fluid flow is inertial or viscous at the grain scale.

When the fluid is a liquid, the density ratio ρ_s/ρ is in the order of unity and the fluid can directly dislodge the grains. Each mobile grain effectuates small displacements of the order of the its diameter, getting momentum from the liquid flow during its displacement, that is later transferred to the interstitial fluid due to its drainage. Finally, a great part of the initial energy is dissipated by the gains dislodgement, by their acceleration, and by the drainage of the interstitial fluid, which is accelerated and generates small scale vortices. The question of the orders of magnitude of these dissipative mechanisms remains open. In the case of liquids, the thickness of this mobile layer is only a few grain diameters.

Also, these dimensionless parameters are, in principle, able to determine the flow rate of grains. However, there are many different formulations for the bed-load flow rate and there isn't a real consensus about it. Besides the different formulae for the bed-load flow rate, there is an extra difficulty, concerning the fluid flow, as it depends on the state of the granular bed (Bagnold, 1941; Raudkivi, 1976; Engelund and Fredsoe, 1982).

Bagnold (1941) showed that the granular transport as bed-load changes the fluid flow. In his classical book about sand transport by the wind, Bagnold showed that the same granular bed, when submitted to the same upstream air flow, generate different air velocity profiles, depending if the grains are all at rest or if a part of them is displaced as bed-load. The main reason for this difference is the momentum transfer from the fluid flow to the mobile grains, and from the latter to the fixed part of the bed (where, in the case of gases, a part of the energy of the moving grains is dissipated by shocks). The change in the fluid flow by the moving grains is usually referred as *feed-back mechanism*.

After the pioneering work of Bagnold (Bagnold, 1936; Bagnold, 1941; Bagnold, 1956), many other experimental works were devoted to measure the feed-back mechanism in air flows (Rasmussen et al, 1996; Bauer et al., 2004; Zhang et al., 2007 and Yang et al., 2007, for instance). In the case of air, as the bed-load thickness is large (many times greater than the grains diameter), it is relatively simple to measure the fluid flow in the mobile layer (and also above it), so that the fluid flow over a mobile granular bed can be compared to that over a fixed one. In general, the posterior experimental results in gas flows corroborate the pioneering work of Bagnold.

In the case of liquids, there are very few experimental works on the feed-back mechanism. Different from gases, in the case of liquids it is very difficult to measure the fluid flow in the mobile layer of grains due to its small thickness (a few grain diameters). To the authors' knowledge, the only experimental work that successfully measured the liquid flow inside the mobile layer of grains (in the case of viscous flows) is Charru et al. (2009). Also, the feed-back effects on the region above the mobile granular layer tend to be smaller than in the case of gases (Raudkivi, 1976; Franklin, 2008), so that it is more difficult to experimentally obtain the perturbation of the liquid flow caused by bed-load.

This work's objective is to assess the effects of the transport of grains as bed-load on a flow of a liquid in turbulent regime. This communication presents an experimental study on the perturbation of a turbulent boundary-layer of a liquid by a mobile granular bed, in conditions close to incipient motion ($\theta \sim 0.01$; Bagnold, 1941; Yalin 1979; Buffington and Montgomery, 1997). An experimental loop was built in which water was employed as the fluid, and loose and fixed glass beads were employed to compose the granular bed. The perturbation caused by the bed-load transport is determined by measuring the velocity profile using PIV (Particle Tracking Velocimetry) in the cases of fixed and mobile granular beds.

The next section presents a summary of the effects of bed-load on the fluid flow. The following section describes the experimental device and procedures. It is then followed by the experimental results and the conclusion sections.

2. EFFECTS OF DENSE GRANULAR MOTION ON THE FLUID FLOW (FEED-BACK MECHANISM)

There are very few experimental studies concerning the influence of the bed-load on a liquid flow. On the other hand, studies on the feed back mechanism in air are more frequent. To better understand this flow phenomenon and to support the experimental data it is developed on the next sub-section a review work on the feed-back mechanism in air. Following this review it is briefed some works and theoretical analysis on the velocity profile when the fluid phase is liquid and the flow regime is turbulent.

2.1. The gas

The pioneering work of Bagnold (Bagnold, 1936; Bagnold, 1941) showed that the granular transport as bed-load changes the fluid flow. Based on experimental results from both wind tunnel and field tests (in the Sahara desert), he showed that the ballistic flights (called *saltation*) of sand grains change the velocity distribution of the wind.

In fact for air transport, distinctly from water transport, the density ratio ρ_s/ρ is large (over *2000)*, implying that, in general, the fluid flow has not enough momentum to directly dislodge the grains. The grains are mainly ejected from the bed by shocks of the falling ones and effectuate ballistic flights whose length-scale is many times greater than the grains diameter, so that the thickness of the mobile layer is many times greater than the grain mean diameter. During the ballistic flight, they get momentum from the gas flow (they are accelerated), and afterwards, when they fall and reach the fixed part of the granular bed, this momentum is transferred again: one part is responsible for the ejection of other grains; other part is dissipated by the shocks; and, if the grain rebound upwards, another part remains with the same grain.

Bagnold (1941) interpreted the momentum transfer to salting grains as a drag caused on the fluid by the moving grains, which profoundly changes the wind velocity distribution near the fixed part of the granular bed, but also changes the upper part of the wind velocity profile. To experimentally arrive to this conclusion, Bagnold measured turbulent air flow profiles over fixed and mobile beds (of same granulometry), subjected to the same upstream air flow, and compared them. The main results are briefly presented on the next paragraphs..

For the fixed granular bed, Bagnold (1941) obtained experimentally turbulent (logarithmic) boundary-layer profiles in the hydraulic rough regime, corresponding to the ones obtained by Nikuradse (1933): they are given by Eq. (2) with roughly $y_0 = d/30$. If the logarithmic profiles are extended towards the origin they will cross each other in a focus where the height and velocity corresponds, respectively to $y = y_0$ *and* $u = 0$.

For the case of a mobile bed, Bagnold (1941) showed the existence of basically two distinct regions:

- A region close to the fixed part of the granular bed, where the bulk of the saltation takes place. In this region, the air velocity distribution suffers a radical change and it is no longer logarithmic. When plotted in the traditional log-normal scales, the velocity profiles present a kink in this region, whose height corresponds to the mean grain path (height reached by the bulk of the saltation). Bagnold (1941) argues that this kink is an experimental evidence of the momentum transfer from the fluid flow to the mobile grains.
- A region above the one where the bulk of the saltation takes place. In this region, the logarithmic velocity profile is re-established, but with a different y_0: as in the case of fixed bed, if the logarithmic profiles are extended downwards, they will cross each other in a focus, corresponding to a height and to a velocity (in the case of the fixed bed, this focus corresponds to $y = y_0$ and $u = 0$). In the case of the moving bed, the focus is located by the intersection between the logarithmic profiles (for different shear velocities) and the line corresponding to the velocity gradient where the sand movement first begins, the *impact threshold* (otherwise the fixed part of the bed would be entrained, please refer to the Appendix). Analyzing the air flow at the inception of sand movement (when the bed is just mobilized by direct entrainment by the fluid, the *fluid threshold*, please refer to the Appendix), Bagnold (1941) observed that at the inception the position of the focus is displaced to a higher position (due to fluid flow deceleration in the saltation region), while the velocity gradient is decreased to the impact threshold value (otherwise the fixed bed would be entrained). The focus is no longer at $u = 0$ and, as the velocity gradient in the upper region increases, the intersection between the velocity gradient line and the line $u = 0$ occurs at a higher positions, i. e., as u_* increases, y_0 also increases.

More recent experimental works on the bed-load effects in gas flows (Rasmussen et al, 1996; Bauer et al., 2004; Zhang et al., 2007 and Yang et al., 2007, for instance) corroborated the original work of Bagnold (Bagnold, 1936; Bagnold, 1941).

2.2. The liquid

As seen in the Introduction section, in the case of liquids the thickness of the mobile layer of grains is of a few grain diameters, very small when compared to gas flows. For this reason, it is very difficult to measure the fluid flow in the mobile layer of grains when the fluid is a liquid. Also, the feed-back effects on the region above the mobile granular layer tend to be smaller than in the case of gases (Raudkivi, 1976; Franklin, 2008), so that it is more difficult to experimentally obtain the perturbation of the liquid flow caused by bed-load. As noted by Bagnold (1941), the density ratio ρ_s/ρ between sand and air is about 2000 and between sand and water about 2. So, if a certain fluid flow dislodge a grain and entrain it to its own velocity, there must be a velocity reduction 1000 times smaller in the case of water when compared to air (subjected by the same bed-load flow rate). Hence, for a given stream and a given bed-load flow rate, the expected deceleration of the stream is 1000 times smaller for water in comparison to air.

The only experimental work that measured the liquid flow inside the mobile layer of grains seems to be Charru et al. (2009), which successfully measured it in the case of viscous flows. The fluid velocity profiles were obtained inside the mobile layer by PIV measurements while the grains were identified by Particle Tracking techniques. In order to obtain the PIV images inside the mobile granular layer, Charru et al. (2009) matched the index of refraction between the fluid (a mixture of two plasticizing liquids) and the acrylic grains. The authors found parabolic profiles with $d^2u/dy^2 > 0$, evidencing the momentum transfer from the fluid to the grains. Whether this parabolic profile is applicable to the fluid flow inside the moving bed in the case of turbulent flows is still to be verified.

In the case of turbulent liquid flows, there is a lack of experimental works concerning the perturbation caused by the bed-load transport. To the authors' knowledge, there are no articles reporting successful measurements of this perturbation.

3. EXPERIMENTAL SET-UP

3.1. Experimental device

An experimental loop was built to study the perturbation caused on a turbulent water stream by the entrainment of grains (as bed-load). To characterize this perturbation, the water flow over fixed and mobile granular beds must be measured, in conditions near the threshold of the bed-load. Figure 1 shows a layout of the experimental loop and a brief description is presented.

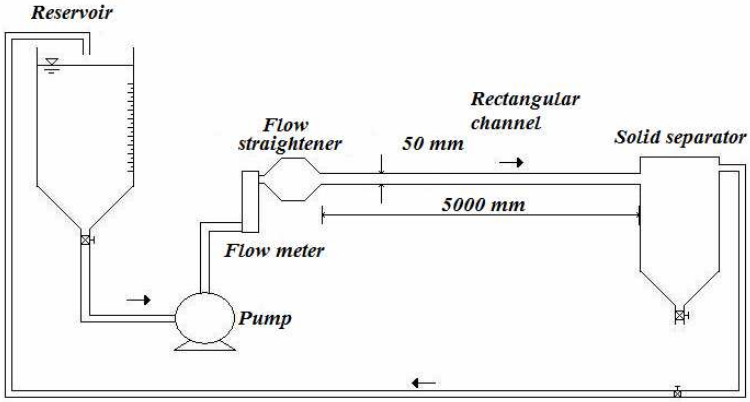

Figure 1. Scheme of the experimental loop

The experimental device consists, basically, of:

- A channel. It is a *5m* long horizontal closed-conduit of rectangular cross-section (*160 mm* wide by *50 mm* high) made of transparent material. The last *2 m* constitute the test section. Access windows ensure the introduction of grains and the formation of the mobile and fixed granular beds.
- A *divergent/honeycomb/convergent device*, located at the channel entrance, whose function is to homogenize the flow and accelerate the process of vortices dissipation. It is composed of a divergent, a honeycomb and a convergent.
- A water reservoir that supplies the channel.
- A recirculation line, that allows the establishment of a closed circuit.

For the construction of a static granular bed, PVC plates (*250 mm* long by *155 mm* wide) were blasted, and glass spheres in the range $d = 300\ \mu m$ to $d = 425\ \mu m$ were glued on their surface. The average thickness of these granular plates was, approximately, *7 mm*. For the fixed bed tests, the plates were introduced in the channel (side by side), covering the entire channel bottom. For the mobile bed tests, the plates were removed (only) in the test section, being replaced by grains of same granulometry, forming a loose granular bed of same thickness.

In order to determine the water flow rate corresponding to the threshold for the bed-load, it was necessary to apply an increasing water flow rate and to observe the beginning of the movement of the grains. All the tests with mobile granular beds were then made at higher water flow rates. The upper limit for the flow rates was imposed by the formation of ripples on the bed surface. Given these limits, the present work concerns water flow rates of approximately *5 m³/h*, *5.5 m³/h*, *6 m³/h*, *6.5 m³/h* and *7 m³/h*.

The tests were performed at approximately atmospheric pressure (*1 atm* or *101325 Pa*) and ambient temperature (*25°C*). The water flow rates of *5 m³/h*, *5.5 m³/h*, *6 m³/h*, *6.5 m³/h* and *7 m³/h* correspond to mean velocities of, respectively, *0.17 m/s*, *0,19m/s*, *0.21 m/s*, *0.23 m/s* and *0,24 m/s*. The Reynolds number based on the hydraulic diameter is in the range $1.32.10^4 < Re < 1.85.10^4$. Three series of tests were performed for the mobile bed case, called here series A, B and C.

3.2. Measurement device: PIV

A LaVision Inc. PIV (Particle Image Velocimetry) device was employed to obtain the flow field velocities. The PIV is a non-intrusive measurement device that obtains instantaneous velocity fields, by optical techniques. Figure 2(a) presents a photo of the PIV device and Fig. 2(b) presents a layout of the PIV apparatus.

The PIV device is composed basically of a laser, a camera, a synchronizer and a software. The laser must be able to generate a laser sheet in a desired plane, illuminating solid particles (seeding particles) whose reflexes are captured, simultaneously, by a camera (the synchrony is assured by the synchronizer). By taking pairs of images, the software computes the most probable displacement field by the cross-correlation of images. Finally, by dividing the displacement field by the time interval, the velocity field is computed.

The employed PIV device was composed of:

- A dual cavity Nd:YAG Q-Switched laser, capable to emit at *2* x *130 mJ* at a *15 Hz* pulse rate. In order to obtain the desired contrasts between the seeding particles and the fluid, avoiding at the same time undesirable reflexes from the channel walls, the power of the laser was fixed between *65%* and *75%*.
- A ImagerProX4M camera, *2048 px* x *2048 px*, with a CCD (charge coupled device) image sensor and capable to acquire pairs of frames at *4Hz*. In our tests, we choose to work with double frame acquisition, and to acquire *500* pairs of images for each flow rate (corresponding then to *500* instantaneous flow fields).
- A synchronizer with *10 ns* time resolution.
- The software DaVis. This software controls the laser shooting, the image acquisitions and performs the images correlations. We employed the DaVis cross-correlations, as we worked with double frame acquisition. The cross-correlations are computed by dividing the images according to a pre-defined mesh (interrogation areas), by taking the FFT (Fast Fourier Transform) of the interrogation areas, by computing their cross-spectrum, and by taking the Inverse Fourier Transform. For each interrogation area, the correlation peak corresponds to the most probable displacement of the seeding particles.

a)

b)

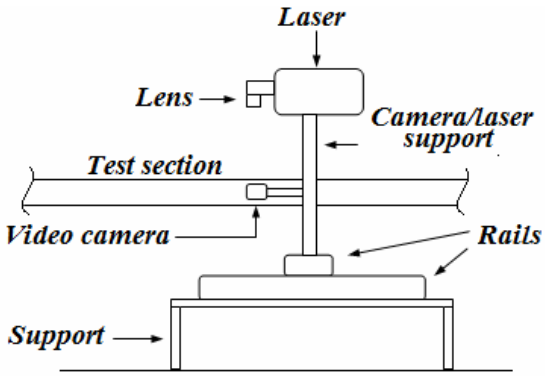

Figure 2. a) Photo of the PIV device ; b) Layout

The PIV is an indirect measurement technique that associates the displacement of solid particles in suspension to the displacement of the fluid particles. For this reason, those solid particles must be passive (passive tracers), i.e., they must follow the fluid flow without perturbing it. As passive tracers, we used the dust already present in the employed tap water, together with hollow glass spheres of $10\ \mu m$ and *S.G. = 1.05*.

The total field employed was *80 mm* x *80 mm* for the tests with fixed bed (note that in the transversal direction, only *50 mm* correspond to the channel height), and *70 mm* x *70 mm* for the tests with mobile beds (again, in the transversal direction only *50 mm* correspond to the channel height). Due to the flow velocities and to the desired interrogation area for the data processing, the time interval between a pair of frames was set to correspond to a maximum displacement of *5 px* of the seeding particles (during this time interval). The employed interrogation area was *8 px* x *8 px*, corresponding then to *256* interrogation areas of *0.28 mm* x *0.28mm*. The computations were made with a *50 %* overlap, increasing the number of interrogation areas to *512*, and the final resolution is then *0.14 mm* x *0.14 mm*.

The software DaVis was employed for the computations of the cross-correlation for each pair of frames, generating then instantaneous velocity fields (*500* fields for each test), but also for the computation of the mean field. The mean field was then post-processed with the MatLab® software.

In order to analyze the flow fields, we needed to determine the correct interface between the fluid flow and the granular bed. However, in the case of a rough bed this cannot be done directly by the pictures of the flow (PIV raw data):

- In the case of granular beds, the glass spheres reflect the laser light in many directions, troubling the identification of the reference height by direct visualization of the images. In this work, the reference height is

considered as the one were mean spatial and temporal profiles reach the zero velocity by post-processing of the mean fields.

- For fixed beds, the reference height was determined for the lower flow rate (*5 m^3/h*) and kept the same for the other flow rates. For mobile beds, a reference height was determined for each test.

3.3 Evaluation of the apparent roughness, of the constant *B* and of the shear velocity

The roughness height y_0 and the shear velocity u_* are determined employing the mean velocity profile obtained experimentally. For this, Eq. (2) is rewritten as

$$u = \frac{u_*}{\kappa}\ln(y) - \frac{u_*}{\kappa}\ln(y_0) \tag{4}$$

where, for a given fluid flow (in our case, a given flow rate) we can identify the constants $A = u_*/\kappa$ and $C = u_*/\kappa\ ln(y_0)$. When plotted in the log-normal scales, the inclination of Eq.(4) is proportional to u_* and the intersection between Eq.(4) and the line $u = 0$ gives y_0. For each water flow condition, the experimental data was fitted to Eq. (4) and the shear velocity and the roughness height were found.

The constant *B* is obtained directly from the right part of Eq. (2), in the same way just described.

4. RESULTS

PIV measurements of the flow field over a fixed granular bed as well as over mobile granular beds were performed. The mean velocity profiles over the fixed and the mobile beds, for roughly the same water flow rates, were compared in order to obtain the perturbation caused by the granular mobility. Due to small variations between setting up the tests and beginning the data acquisition, but also to the large response time of the electromagnetic flow-meter, the water flow rates showed here were obtained from the integration of the PIV measured profiles.

Figure 3 presents the mean velocity profiles over fixed and mobile granular beds, subjected to roughly the same water flow rates. The employed symbols are listed in Tab. 1 and the scales are linear. Figure 3(a) corresponds to, roughly, a water flow rate of *5 m^3/h*, Fig. 3(b) to a water flow rate of *5.5 m^3/h*, Fig. 3(c) to a water flow rate of *6 m^3/h* and Fig. 3(d) to a water flow rate of *6.5 m^3/h*.

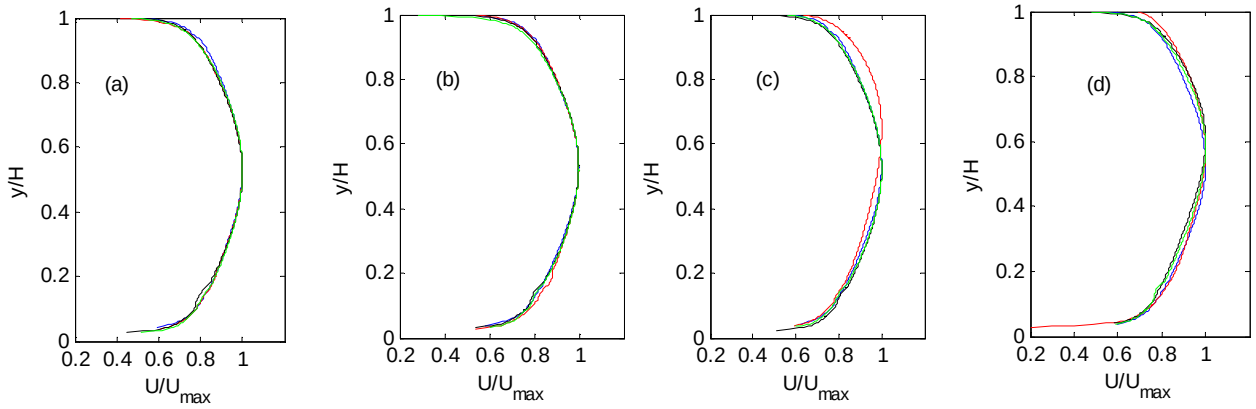

Figure 3. Mean velocity profiles normalized by their maxima over fixed and mobile granular beds, subjected to, approximately, the same water flow rates: a) *5 m³/h*; b) *5.5 m³/h;* c) *6 m³/h*; d) *6.5 m³/h*. *H* is the distance between the granular bed and the top wall. The list of the employed colors as well as the maxima values are presented in Tab. 1.

The bed-load threshold is close to a water flow rate of *5 m³/h*. At this condition, it is expected that the density of mobile grains (the rate of mobile to static grains) is low, causing then a very small effect on the water stream. This is what the measurements indicate, as can be observed from Figs. 3(a) and 3(b). In these figures, we can see that the profiles are almost superposed, indicating little effect of bed-load on the water stream. In fact, in Fig. 3 they are not perfectly superposed because the flow rate was slightly smaller in the fixed bed case (cf. Tab. 1). We note here that the kinks seen in $y/H \approx 0.14$ and in $y/H \approx 0.95$ for some of the profiles come from instrumentation problems (saturation of the PIV images in this region caused by undesired reflexes).

As the water flow rate is increased, we go far from the bed-load mobility and the density of mobile grains increases, causing an increase in the effect on the water stream. This is shown in Fig. 3(c) and in Fig. 3(d). In these figures, some of the profiles over mobile beds (two in Fig. 3(c) and all in Fig. 3(d)) have an increased asymmetry, indicating an increased water flow resistance over the mobile bed. For even important flow rates, as the density of mobile grains increases, this equivalent roughness is expected to increase. Figure 4 presents the comparison between the flow over

fixed and mobile beds for *7 m³/h* (reached only in series B). It can be seen that the asymmetry is even stronger, indicating the effect of an increased water flow resistance over the mobile bed.

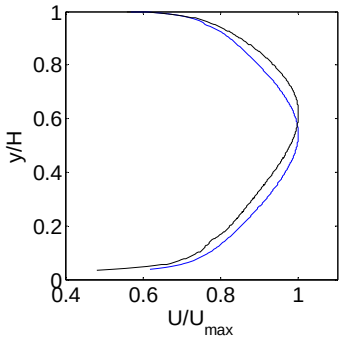

Figure 4. Mean velocity profiles normalized by their maxima over fixed and mobile granular beds, subjected to, approximately, the same water flow rates of *7 m³/h*. *H* is the distance between the granular bed and the top wall. The list of the employed colors as well as the maxima values are presented in Tab. 1.

Based on the original work of Bagnold (1941), we can expect the existence of a turbulent boundary-layer over the mobile bed, with a region in which the mean velocity has a logarithmic profile. For this reason, we present in Fig. 5 the mean velocity profiles over fixed and mobile granular beds, subjected to the same water flow rates, in the traditional log-normal scales. In these figures, the mean velocity is normalized by the shear velocity $u^+ = u/u_*$ and the transversal distance is normalized by the viscous length $y^+ = yu_*/\nu$.The employed symbols are listed in Tab. 1. Figure 5(a) corresponds to series A, Fig. 5(b) to series B and Fig. 5(c) to series C.

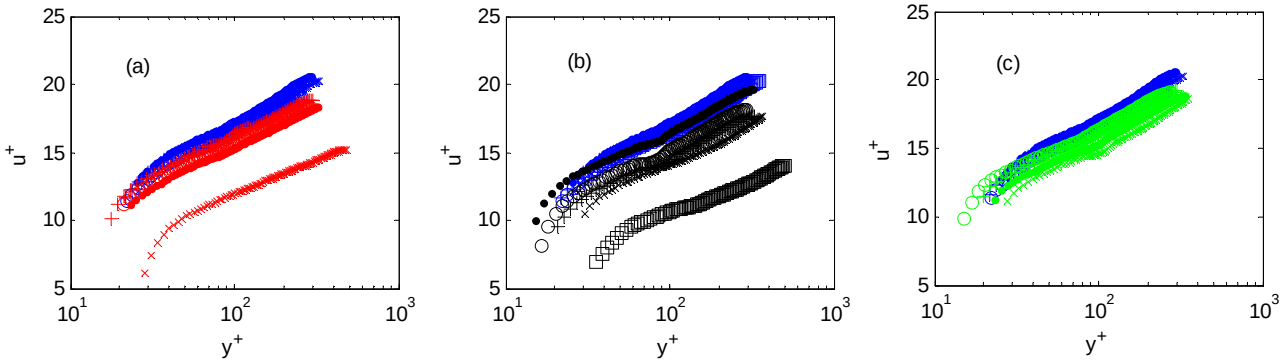

Figure 5. Mean velocity profiles over fixed and mobile granular beds, normalized by the internal scales (shear velocity and viscous length). The abscissa is in logarithmic scales. The employed symbols are listed in Tab. 1: (a) corresponds to series A, (b) corresponds to series B and (c) corresponds to series C.

The normalized profiles for the flow over a fixed bed are almost superposed. In fact, the boundary-layer is in the hydraulic smooth regime (or in the beginning of the transitions), as can be verified by the values of Re_* presented in Tab.1 (Schlichting, 2000). Given this regime, the values of u_* and the origin ($y = 0$) where obtained by fitting the profiles in order to obtain $B = 5.5$.

Comparing the profiles over the mobile beds with the ones over a fixed bed, we observe that the profiles are similar: they present a logarithmic region above the bed. However, the profiles over mobile beds are displaced to higher locations (the same velocities are reached at higher transversal coordinates), and this displacement increases as the granular mobility is increased.

The agreement of these profiles with Eq. (2) in a region close to the granular bed indicates that the flow is in local equilibrium in this region. The same occurs close to the top wall (not shown here), and the interaction between the two near-wall regions seems to occur at the central region (although not exactly at the center of the channel, there is an asymmetry). This behavior was experimentally measured by Hanjalic and Launder (1972) in the case of asymmetric two-dimensional channels, with fixed beds (in the hydraulic rough regime). The same seems to happen in the case of a mobile bed. For this reason, we analyze here only the effects of the bed-load on the near granular bed region, leaving the discussion on the central region and on the upper wall to be done in a future opportunity.

Bagnold (1941) postulated, in the case of hydraulic rough gas flows, that the influence of the bed-load on the mean flow can be regarded as the generation of an *effective roughness* which is greater than the one expected for a fixed granular bed of same granulometry. He also postulated that the cause of the increase in the effective roughness with the

granular mobility is the momentum transfer from the fluid to the mobile grains, which is then "lost" by dissipative mechanisms (shocks, in the case of gases).

In the case of water, the higher density of the fluid means a lower velocity reduction for the same momentum transfer, but also that the grain has a smaller relative weight (in comparison to air). This means that, given a loose granular bed, the bed-load threshold occurs at lower velocity gradients (and lower velocities), so that it can happen in the hydraulic smooth regime. Although in our experiments the water boundary-layer was hydraulic smooth, Fig.5 shows a displacement of the normalized profiles that increases with grains mobility, very similar to the aeolian (hydraulic rough) case.

For liquid flows in the hydraulic smooth regime, we postulate that the feed-back effects are similar to the one proposed by Bagnold (1941): the momentum transfer from the fluid to the mobile grains decelerates the liquid in the region near the bed, displacing the water flow profiles but keeping the same normalized form. This displacement increases with granular mobility (and with the water flow rates), due to an increase in the momentum transfer from the fluid to the mobile grains, which is then "lost" by dissipative mechanisms. In the case of liquids, a great part of the initial energy is dissipated by the gains dislodgement, by their acceleration, and by the drainage of the interstitial fluid, which is accelerated and generates small scale vortices. This displacement would be equivalent to an increase in the *effective roughness*, but care must be made as the water flow is in the hydraulic smooth case (cf. Tab.1).

If one effect of the mobility on the water stream is the displacement of the turbulent boundary-layer, then a logarithmic layer given by Eq. (2) shall exist, however with a different value of the B constant, or a different value of the roughness height y_0 (the two sides of Eq. 2 are equivalent as $y_0 = (\nu/u_*)e^{-\kappa B}$). For flows over fixed beds in hydraulic smooth regime, $B = 5.5$ (Schlichting, 2000). The measured water flows over the fixed bed lie in this case. For flows over mobile beds, the values of B shall be different, and vary with the granular mobility.

Considering the logarithmic region in the measured water profiles, the shear velocity u_*, the constant B and the roughness height y_0, for both the fixed and mobile beds, can be estimated as described in subsection 3.3. Table 1 presents a summary of these estimations.

Table 1. Shear velocity u_*, roughness height y_0 and constant B estimation. "Fix" stands for fixed bed and "mob A", "mob B" and "mob C" stand for, respectively, the three series of tests with mobile beds, called here "A", "B" and "C". The column "symbol" lists the colors employed in Figs. 3, 4 and the symbols employed in Fig. 5. Q is the water flow rate computed from the measured PIV profiles, U_{max} is the maximum water velocity in each profile, Re_* is the particular Reynolds number (defined in Eq. 3) and θ is the Shields number (defined in Eq. 1).

	Q (m3/h)	symbol	B	y0	u* (m/s)	Umax (m/s)	Re*	θ
fix	5.0	o	5.30	d/37	0.0117	0.22	4	0.03
	5.6	+	5.70	d/47	0.0126	0.25	5	0.03
	6.1	.	6.00	d/57	0.0134	0.28	5	0.03
	6.8	x	5.20	d/47	0.0150	0.30	5	0.04
	7.3	□	5.20	d/50	0.0161	0.33	6	0.05
mob A	5.3	o	4.40	d/28	0.0130	0.24	5	0.03
	5.8	+	5.00	d/38	0.0136	0.26	5	0.03
	6.1	.	4.10	d/29	0.0145	0.27	5	0.04
	6.8	x	2.90	d/21	0.0171	0.30	6	0.05
mob B	5.3	o	3.90	d/24	0.0133	0.24	5	0.03
	5.9	+	3.40	d/22	0.0149	0.26	5	0.04
	6.3	.	5.30	d/46	0.0145	0.29	5	0.04
	6.7	x	3.00	d/21	0.0168	0.30	6	0.05
	7.3	□	-0.50	d/7	0.0228	0.33	8	0.10
mob C	5.4	o	5.10	d/37	0.0126	0.24	5	0.03
	5.9	+	5.00	d/38	0.0136	0.26	5	0.03
	6.4	.	4.30	d/32	0.0153	0.29	6	0.04
	6.8	x	3.80	d/27	0.0162	0.31	6	0.05

For the fixed bed we found, as expected, that the shear velocity u_* increases with the water flow rate, and that the constant B does not vary with the water flow. The experimental data was fitted to give an approximate value of *5.5* to B.

Concerning the mobile beds, we note that for some flow rates (*5* and *5.5* m^3/h) the values of B and u_* are almost unchanged with respect to the fixed bed. It is probable that by the time the PIV measurements were taken, the bed became static due to *armouring* effects (please see the Appendix). This is confirmed by the values of the Shields number calculated for these cases: $\theta \leq 0.04$, knowing that the threshold value is $\theta \approx 0.04$ (Yalin 1979; Buffington and Montgomery, 1997; Charru et al., 2004). Above the threshold, the shear velocity u_* increases while the constant B decreases, in comparison to the flow over a fixed bed. Also, the constant B decreases with the increasing in the water flow rate.

These variations may be explained as follows. Close to the bed, in the saltation layer, the fluid flow is strongly affected by the mobile grains. In this layer, the fluid flow transfers momentum to the mobile grains, and a part of this momentum is lost by dissipative processes. The effect on the water flow of this momentum transfer is a strong slow

down in the region close to the saltation layer. Well above the saltation layer, in the core flow, the water flow is less affected by the saltation layer (if compared to a flow over a fixed bed of same granulometry). This implies that in this region the mean velocity profiles shall be similar to the ones over a fixed bed.

We postulate here that, as in the aeolian case (Bagnold, 1941), the profile of a liquid flow over a mobile bed is constituted of: (a) a *lower region* ($y^+<40$), close to the saltation layer, where the effects of momentum transfer are very strong and slow down the liquid flow; (b) an *upper region* ($y^+>200$), far enough from the saltation layer (near the core flow) so that the mean fluid flow shall have a profile similar to the one over a fixed bed (of same granulometry); and (c) a *matching region* ($50<y^+<150$) which, as in the case of turbulent boundary-layers over fixed granular beds, shall have a logarithmic profile. These three regions can be seen in Fig. 5.

In the case of closed-conduit flows, the flow in the *upper region* (core flow) changes slightly, different from open flows. In the case of bed-load transport in closed-conduits, the slow down in the *lower region* implies, by mass conservation, an acceleration in the *upper region* and an increase in the asymmetry. If the fluid flow is near the bed-load threshold, the momentum transfer in the *lower region* is relatively small, so that the deceleration near the bed and the acceleration in the core flow are barely noticed, and the shear velocity is almost the same as in the case of a fixed bed. As the fluid flow rate is increased, the density of mobile grains increases and there is an increase in the momentum transfer near the bed: the slow down near the bed and, consequently, the acceleration in the core flow increase the shear velocity in both walls. Also, the slow down in the *lower region* displace the entire logarithmic layer to higher transversal positions, corresponding to the lower values measured for the *B* constant. In this work we analyzed only the effects in the region near the granular bed, so that we didn't report the variation of u_* in the top wall. The discussion on the upper wall is left to a future opportunity.

Based on the above observations, we propose, although in the hydraulic smooth regime, that the bed-load effect on the fluid flow is similar to an increase in the roughness height y_0, but keeping the general fluid flow profile.

5. CONCLUSION

This communication was devoted to understand the effects on a turbulent fluid flow by the transport of grains as bed-load, when the fluid is a liquid. We presented an experimental study on the perturbation of a turbulent boundary-layer of a liquid by a mobile granular bed, in conditions close to incipient motion. An experimental loop was built with water as the liquid phase and glass beads as the granular media composing the bed, which was static or mobile. The velocity field of the water stream was measured by PIV (Particle Tracking Velocimetry) in the cases of static and mobile granular beds, and the perturbation caused by the bed-load transport could be determined.

We successfully measured the perturbation caused on the turbulent stream by the bed-load. The good agreement between the measured profiles and the law of the wall in the region close to the granular bed indicates that the flow is in local equilibrium in this region. The same occurs close to the top wall and the interaction between the two near-wall regions occurs at the central region. We analyzed in this paper only the effects of the bed-load on granular bed region, leaving the discussion on the central region and on the top wall to be done in a future opportunity.

Our measurements indicate the existence of at least three distinct regions in the mean water flow: one region near the saltation layer, where the flow is strongly slowed down due to momentum transfer, called here *lower region;* a region far from the granular bed and near the core flow, where the perturbation effects are weaker (the mean fluid flow shall have a profile similar to the one over a fixed bed), called here *upper region*; and an intermediate region, which must match the *upper* and the *lower* ones, and then shall have a logarithmic profile, called here *matching region*. Also, based on this observation, we propose, as for the aeolian case (Bagnold, 1941), that the bed-load effect on the fluid flow is similar to an increase in the roughness height y_0, but keeping the general fluid flow profile.

6. ACKNOWLEDGEMENTS

The authors are grateful to Petrobras S.A. for the financial support (contract number 0050.0045763.08.4), including the scholarship granted to Fabíola Tocchini de Figueiredo.

7. REFERENCES

Bagnold, R.A., 1936, "The movement of desert sand", Proc. R. Soc. Lond. A, Vol. 157, pp. 594-620.

Bagnold, R.A., 1941, "The physics of blown sand and desert dunes", Ed. Chapman and Hall, London, United Kingdom, 320 p.

Bagnold, R.A., 1956, "The flow of cohesionless grains in fluids", Philos. Trans. R. Soc. Lond. Ser. A, Vol. 249, pp. 235-297.

Bauer, B.O., Houser, C.A. and Nickling, W.G., 2004, "Analysis of velocity profile measurements from wind-tunnel experiments with saltation", Geomorphology, Vol. 59, pp. 81-98.

Buffington, J.M. and Montgomery, D.R., 1997, "A systematic analysis of eight decades of incipient motion studies, with special reference to gravel-bedded rivers", Water Resour. Res., Vol.33, pp. 1993-2029.

Charru, F., Mouilleron-Arnould, H. and Eiff, O., 2004, "Erosion and deposition of particles on a bed sheared by a viscous flow", J. Fluid Mech., Vol. 519, pp. 55 - 80.
Charru, F., Mouilleron-Arnould, H. and Eiff, O., 2009, "Inside the moving layer of a sheared granular bed", J. Fluid Mech., Vol. 629, pp. 229-239.
Engelund, F. and Fredsoe, J., 1982, "Sediment ripples and dunes", Ann. Rev. Fluid Mech., Vol. 14, pp. 13 - 37.
Franklin, E.M., 2008, "Dynamique de dunes isolées dans un écoulement cisaillé", (in french), Ph.D. Thesis, Université de Toulouse, Toulouse, France, 166 p.
Hanjalic, K. and Launder, B.E., 1972, "Fully developed asymetric flow in a plane channel", J. Fluid Mech., Vol. 51, pp. 301-335.
Nikuradse, J., 1933, "Strömungsgesetze in rauhen rohren", VDI Forschungsh., Vol 361 ; English trans., NACA Tech. Mem. 1292.
Raudkivi, A.J., 1976, "Loose boundary hydraulics", Ed. Pergamon, Oxford, United Kingdom, 397p.
Rasmunsen, K.R., Iversen, J.D. and Rautahemio, P., 1996, "Saltation and Wind-flow interaction in a variable slope wind tunnel", Geomorphology, Vol. 17, pp. 19-28.
Schlichting, H, 2000, "Boundary-layer theory", Ed. Springer, Berlin, Germany, 801p.
Yalin, M.S., 1977, "Mechanics of sediment transport", Ed. Pergamon Press, Oxford, United Kingdon, 298p.
Yalin, M.S., 1979, "Inception of sediment transport", J. Hydraul. Div., Vol.HY11, pp. 1433-1443.
Yang, P., Dong, Z., Qian, G., Luo, W. and Wang, H., 2007, "Height profile of the mean velocity of an aeolian salting cloud: Wind tunnel measurements by Particle Image Velocimetry", Geomorphology, Vol. 89, pp. 320-334.
Zang, W., Wang, Y. and Lee, S.J., 2007, "Two-phase measurements of wind and salting sand in atmospheric boundary layer", Geomorphology, Vol. 88, pp. 109-119.

8. RESPONSIBILITY NOTICE

The authors are the only responsible for the printed material included in this paper.

9. APPENDIX: INCEPTION OF BED-LOAD TRANSPORT

In the case of gas flows, Bagnold (Bagnold, 1936 and Bagnold, 1941) showed the existence of two critical wind strengths for the inception of granular movement on an initially static bed. The higher one, called *Fluid Threshold*, corresponds to the inception of the sand transport directly by the fluid flow (in the case of gases, by pressure drag on grains). This threshold has not a definite value as it depends on the presence of exposed individual grains (i.e., on the bed compactness) and on eddies, in the case of turbulent flows.

The lower one, called *Impact Threshold*, was defined by Bagnold as "the critical threshold wind at which an initial disturbance of the sand becomes a continuous movement along the down-wind surface (…)" (Bagnold, 1941, page 32). In other words, if some external disturbance initiates the movement of some grains at a given location, those grains get momentum from the fluid flow and, if the flow is above the impact threshold, the granular movement will continue downstream.

Due to these two distinct thresholds, hysteresis is observed between the inception and the stop of saltation in gas flows. Departing from a fixed bed and increasing the gas flow velocities, the bed-load transport will begin when the fluid threshold is reached. At this threshold, the granular transport will be sustained because the impact threshold is lower. If the gas flow velocities are reduced, bed-load will continue as far as the conditions are above the impact threshold: granular transport will only stop at fluid velocities below the impact threshold. Bagnold (1941) also showed that when the fluid threshold is reached, the shear stress on the bed drops to the impact threshold value, otherwise the fixed part of the bed would be entrained.

In the case of liquids, there are no ejection of grains by shocks (the interstitial fluid dumps the shocks) so that the impact threshold no longer exists: there is only the fluid threshold. However, its determination is not simple due to the time variation of the compactness of the bed, called *armouring*. In liquids, the impacts between grains are dumped by the interstitial fluid so that there is no mechanism to maintain the bed loose, while the movement of grains tends to compact the bed by a trapping effect (armouring).

Consider an initially loose granular bed submitted to a liquid flow just above the fluid threshold. As a consequence of the armouring, after some (characteristic) time the granular bed will be more compact and the more exposed grains will be trapped. So, in order dislodge some grains, the liquid flow must increase to a higher value, meaning a new fluid threshold. This situation will continue as long as armouring happens, i. e., it will stop when the granular bed reach its maximum compactness. The conclusion is that, in the case of liquids, the fluid threshold is strongly dependent on the initial state of the granular bed. Experimental evidences of armouring for bed-load in a viscous flow can be seen in Charru et al. (2004).